

Detecting Multi-Sensor Fusion Errors in Advanced Driver-Assistance Systems

Ziyuan Zhong

ziyuan.zhong@columbia.edu
Columbia University
USA

Xinyang Zhang

xinyangzhang@baidu.com
Baidu Security
USA

Zhisheng Hu

zhishenghu@baidu.com
Baidu Security
USA

Shengjian Guo

sjguo@baidu.com
Baidu Security
USA

Zhenyu Zhong

edwardzhong@baidu.com
Baidu Security
USA

Baishakhi Ray

rayb@cs.columbia.edu
Columbia University
USA

ABSTRACT

Advanced Driver-Assistance Systems (ADAS) have been thriving and widely deployed in recent years. In general, these systems receive sensor data, compute driving decisions, and output control signals to the vehicles. To smooth out the uncertainties brought by sensor inputs, they usually leverage **multi-sensor fusion** (MSF) to fuse the sensor inputs and produce a more reliable understanding of the surroundings. However, MSF cannot completely eliminate the uncertainties since it lacks the knowledge about which sensor provides the most accurate data and how to optimally integrate the data provided by the sensors. As a result, critical consequences might happen unexpectedly. In this work, we observed that the popular MSF methods in an industry-grade ADAS can mislead the car control and result in serious safety hazards. Misbehavior can happen regardless of the used fusion methods and the accurate data from at least one sensor. We call such errors as fusion errors and develop a novel evolutionary-based domain-specific search framework, *FusED*, for the efficient detection of fusion errors. We further apply causality analysis to show that the found fusion errors are indeed caused by the MSF method. We evaluate our framework on two widely used MSF methods in two driving environments. Experimental results show that *FusED* identifies more than 150 fusion errors. Finally, we provide several suggestions to improve the MSF methods we study.

KEYWORDS

advanced driving assistance system, testing, causality

ACM Reference Format:

Ziyuan Zhong, Zhisheng Hu, Shengjian Guo, Xinyang Zhang, Zhenyu Zhong, and Baishakhi Ray. 2022. Detecting Multi-Sensor Fusion Errors in Advanced Driver-Assistance Systems.

1 INTRODUCTION

Advanced Driver-Assistance Systems (ADAS) are human-machine systems that assist drivers in driving and parking functions and have been widely deployed on production passenger vehicles [6] (e.g. Tesla’s AutoPilot, Cadillac’s Super Cruise, and Comma Two’s OPENPILOT [24]). Unlike the full automation promised by so-called self-driving cars, ADAS provides partial automation like adaptive

cruise control, lane departure warning, traffic signals recognition, etc., to promote a safe and effortless driving experience. Although ADAS are developed to increase road safety, they can malfunction and lead to critical consequences[1]. It is thus important to improve the reliability of ADAS.

A typical ADAS, as shown in Figure 1, takes inputs from a set of sensors (e.g., camera, radar, etc.) and outputs driving decisions to the controlled vehicle. It usually has a perception module that interprets the sensor data to understand the surroundings, a planning module that plans the vehicle’s successive trajectory, and a control module that makes concrete actuator control signals to drive the vehicle. Oftentimes individual sensor data could be unreliable under various extreme environments. For example, a camera can fail miserably in a dark environment, in which a radar can function correctly. In contrast, a radar can miss some small moving objects due to its low resolution, while a camera usually provides precise measurements in such cases. To enable an ADAS to drive reliably in most environments, researchers have adopted complementary sensors and developed multi-sensor fusion (MSF) methods to aggregate the data from multiple sensors to model the environment more reliably. If a sensor fails, MSF can still work with other sensors to provide reliable information for the downstream modules and enable the ADAS to operate safely.

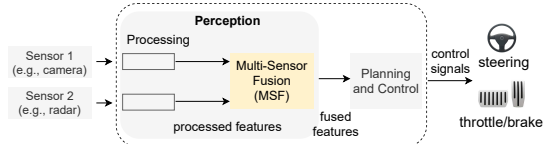


Figure 1: The architecture of a typical ADAS system.

However, an MSF hardly knows which sensor input to rely on at each time step. Thus, it neither thoroughly eliminates the uncertainty nor always weighs more on the correct sensor data. This inherent flaw may introduce safety risks to the ADAS. In this paper, we study a popular commercial ADAS named OPENPILOT and show that sometimes its MSF can prioritize faulty sensor information over the correct ones. Thus, even if alternative sensors may provide more accurate information, incorrect fusion logic can lead the vehicle to critical accidents. To this end, this paper focuses on automatically detecting accidents (i.e., collisions) that can occur due to incorrect fusion logic—we call such accidents as *fusion errors*.

Similar to existing ADAS testing[2–4], we resort to simulation rather than real-world testing as the latter is prohibitively expensive. A vehicle controlled by the ADAS, also known as the *ego car*, drives through the scenario generated by a high-fidelity simulator. Here, the MSF logic of the ADAS is under test. The semantic validity of the generated scenarios are guaranteed by the usage of the simulator’s traffic manager which controls other vehicles (not controlled by ADAS) to behave in a realistic way. Our aim is to simulate scenarios that facilitate fusion errors in the ADAS. However, detecting fusion errors even in a simulated environment is challenging.

Challenges. First, existing fusion methods can function properly most of the time, so their failure cases are sparse among all the driving situations. Given testing an AD system is costly, it is non-trivial to identify sparsified failure cases within a limited time budget. Second, even if we detect an accident, it is hard to conclude its root cause is incorrect fusion logic. Employing simple differential testing even if we simulate the whole driving scenario with alternative fusion logic and avoid the collision, we cannot say with certainty that the root cause was the faulty fusion logic. This is because many uncertainties are involved in the end-to-end ADAS system—non-deterministic sensor inputs, random time delays between simulator and controller, etc., reproducing the exact collision is non-trivial.

Our Approach. A fusion error takes place (i) when the output of two sensors differs significantly, and (ii) the fusion logic chooses the wrong sensor output even though the correct output is available. To detect such errors, we first use fuzz testing that promotes two sensors to behave differently under the same environment. If a crash happens, we further apply root cause analysis to filter out the errors that may not have been caused by faulty fusion logic. We realize these steps using a tool *FusED* (*Fusion Error Detector*).

Fuzzing. In order to induce fusion errors, the simulator needs to generate scenarios that promote the fusion component to provide inaccurate prediction although the non-chosen sensor output provides accurate prediction. In the driving automation testing domain, recent works leverage fuzz testing to simulate input scenarios in which an ego car runs and the fuzzer is optimized to search for failure-inducing scenarios [2, 23, 31, 50]. However, these methods treat the ego-car system as a black-box and ignore the attainable runtime information of the system. Inspired by the grey-box fuzzing of traditional software fuzzing literature [35], we propose an evolutionary algorithm-based fuzzing that utilizes the input and output information of the fusion component of the system. In particular, we propose a novel objective function that maximizes the difference between the fusion component’s prediction and the ground-truth, while minimizing the difference between the most accurate sensor’s prediction and the ground-truth. Here, ground-truth is the actual relative location and relative speed of the leading vehicle w.r.t. the ego-car. If the simulation then witnesses a collision of the ego car, it is highly likely the fusion logic chooses the wrong output over the correct one.

Root Cause Analysis. To check whether the observed collision is indeed due to the fusion logic, we study if the error still happens after choosing an alternate fusion logic in an otherwise identical simulation environment. However, maintaining an identical setting is infeasible because of many uncertainties and randomness in the simulator and controller environment. Thus, we rely on the theory of causal analysis. Based on domain knowledge, we construct

a causal graph, where graph nodes are all the variables that can influence the occurrence of a collision during a simulation, and the edges are links that show their influence with each other. We then intervene and change the fusion logic by keeping all the other nodes identical in the causal graph. Such intervention is applied by setting the communications between the simulator and ego-car deterministic and synchronous for all the simulations. To efficiently find a fusion method that can avoid the collision, we use a *best-sensor fusion* method, which always selects the sensor’s output that is closest to the ground truth. If we no longer see the collision in this counterfactual world, we conclude that the root cause of the observed collision was incorrect fusion logic. Otherwise, we discard the error. To further reduce double-counting the same error, we propose a new fusion errors counting metric based on the coverage of the ego car’s location and speed trajectory during each simulation.

To the best of our knowledge, our technique is the first fuzzing method targeting the ADAS fusion component. In total, *FusED* has found more than 150 fusion errors. In summary, we make the following contributions:

- We define *fusion errors* and develop a novel grey-box fuzzing technique for efficiently revealing the *fusion errors* in ADAS.
- We analyze the root causes of the *fusion errors* using causality analysis.
- We evaluate *FusED* in an industry-grade ADAS, and show that it can disclose safety issues.
- We propose suggestions to mitigate *fusion errors* and effectively reduce *fusion errors* in a preliminary study.

2 BACKGROUND: FUSION IN ADAS

The "Standard Road Motor Vehicle Driving Automation System Classification and Definition" [25] categorizes driving automation systems into six levels. Advanced Driver-Assistance Systems (ADAS) usually consists of levels 0 to 2, which only provides temporary intervention (e.g., Autonomous Emergency Braking (AEB)) or longitudinal/latitudinal control (e.g., Automated Lane Centering (ALC) and Adaptive Cruise Control (ACC)) while requiring the driver’s attention all the time. In contrast, Automated Driving Systems (ADS) consist of levels 3 to 5, which allow the driver to not pay attention all the time. In this section, we introduce commonly used fusion methods and related errors for driving automation systems. In particular, we focus on OPENPILOT, a level2 industry-grade ADAS. However, we believe our approach can also generalize to ADS that use similar fusion methods [9, 43].

We next define the terminologies used later. A *driving environment* is a parameterized space where search during the fuzzing will be bounded. A *scenario* is a concrete instance in the driving environment. The *ego car* is the vehicle controlled by the ADAS under test. The *NPC (non-player character) vehicles* are the vehicles other than the ego car in the scenario. The *leading vehicle* is the vehicle ahead of the ego car in the same lane. A high-fidelity *simulator* provides an end-to-end simulation environment for testing ADAS. It generates sensor data at regular intervals (from cameras, radar, etc.) that can be fed into the ADAS under test, and receives control signal from the ADAS to update the ego car in the simulated world.

2.1 Fusion in Driving Automation

Most industry-grade driving automation systems, including ADAS and ADS, leverage multi-sensor fusion (MSF) to avoid potential accidents caused by the failure of a single sensor [9, 15, 43]. MSF often works with camera and radar, camera and Lidar, or the combination of camera, radar, and Lidar [48]. There are three primary types of MSF: high-level fusion (HLF), mid-level fusion (MLF), and low-level fusion (LLF). They differ in how the data from different sensors are combined. In HLF, each sensor independently carries out object detection or a tracking algorithm. The fusion is then conducted on the high-level object attributes of the environment (e.g., the relative positions of nearby vehicles) provided by each sensor and outputs aggregate object attributes to its downstream components. LLF fuses the sensor data at the lowest level of abstraction (raw data)[49]. MLF is an abstraction-level between HLF and LLF. It fuses features extracted from the sensor data, such as color information from images or location features of radar and LiDAR, and then conducts recognition and classification on them[32]. Among them, HLF is widely used in open-sourced commercial-grade ADAS [15] or ADS [9, 43] because of its simplicity. Thus, it is the focus of the current work. In particular, we conduct a CARLA simulator-based case study on an industry-grade ADAS, OPENPILOT, which uses an HLF for camera and radar.

2.2 Fusion in OPENPILOT

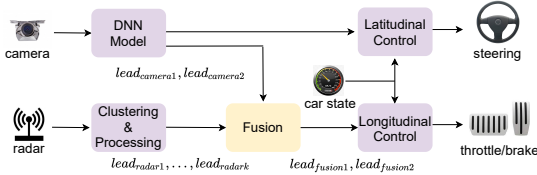


Figure 2: The role of fusion in OPENPILOT.

Figure 2 shows the the fusion component in OPENPILOT. It receives data about the leading vehicles from the camera processing component and the radar processing component. Each leading vehicle data, denoted as *lead*, consists of the relative speed, relative longitudinal and latitudinal distances to the leading vehicle, and the confidence of this prediction (only for camera). The fusion component aggregates all lead information from the upstream sensor processing modules and outputs an estimation to the longitudinal control component. Finally, the longitudinal control component outputs the decisions for throttle and brake to control the vehicle. Note that the latitudinal control component only relies on camera data so we do not consider accidents due to the auto-driving car driving out of the lane. Different fusion logics can be implemented. Here we studied OPENPILOT default one and a popular Kalman-Filter-based fusion method [33, 36].

DEFAULT: Heuristic Rule-based Fusion. Figure 3a shows the logic flow of the OPENPILOT’s fusion method DEFAULT. It first checks if the ego car’s speed is *low*($ego_speed < 4$) and *close* to any leading vehicle (①). If so, the closest radar leads are returned. Otherwise, it checks if the *confidence* of any camera leads go beyond 50% (②). If not, leading vehicles will be considered non-existent. Otherwise, it checks if any radar leads match the camera leads (③). If so, the best-matching radar leads are returned. Otherwise, the camera leads are returned.

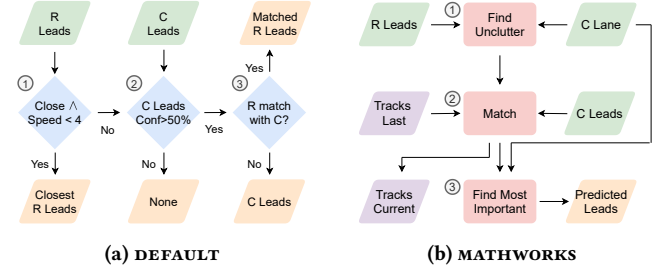


Figure 3: Fusion logic of (a)OPENPILOT DEFAULT and (b)MATHWORKS. C denotes camera and R denotes radar. Green, orange, blue, red, and purple denote input, output, decision, processing, and stored data over generations, respectively.

MATHWORKS: Kalman-Filter Based Fusion. Figure 3b shows the logic of MATHWORKS which is a popular fusion method from Mathwork[36]. It starts with the camera-predicted lane to filter out cluttered (i.e. stationary outside the ego car’s lane) radar leads in ①. Then, it groups together camera leads and uncluttered radar leads, and matches them with tracked objects from last generation in ②. Tracked objects are then updated. Finally, matched tracked objects within the current lane are ranked according to their relative longitudinal distances in ③ and the data of the closest two leads are returned.

2.3 A Fusion Error Example

The fusion module sometimes makes an error when there is a disagreement between different sensor inputs, and the underlying fusion logic trusts the faulty sensor input. Following is a motivating example of fusion misbehavior inducing accident of OPENPILOT.

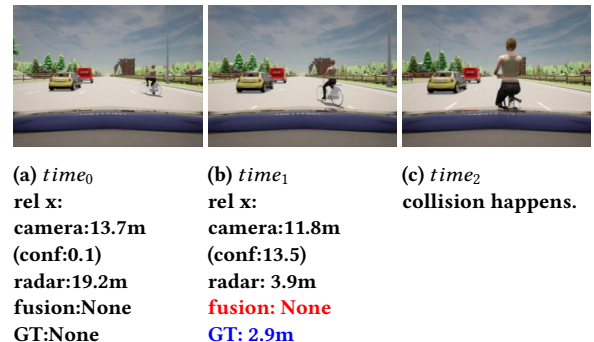


Figure 4: A collision example. The ego car is the blue car from whose viewing angle rest of the environment can be seen. *rel x*: relative longitudinal distance of the ego car from the cycle. GT: the ground-truth value. The fusion error and GT are highlighted in red and blue respectively.

Motivating Example. Figure 4 shows an example where the ego car collides with a bicyclist cutting in. At *time*₀ (Figure 4a), no leading vehicle exists. At *time*₁ (Figure 4b), the bicyclist on the right trying to cut in. While the radar predicts that the lead is close (3.9 m) to the ground-truth value (2.9m), the camera ignores the bicyclist. The fusion component trusts the camera so the ego car does not slow down, and finally a collision occurs at *time*₂(Figure 4c). This example shows an accident caused by a wrong result from the fusion component. But how could the problem happen?

In the logic flow of the OPENPILOT’s DEFAULT fusion method (see Figure 3a), due to path (1) and (2), i.e., $\neg(\text{ego_speed} < 4 \wedge \text{close})$ and $\neg(\text{camera confidence} > 50\%)$, no leading vehicle is considered existent at $time_1$ (i.e., Fusion output=None). Thus, the ego car accelerates until hitting the bicyclist.

3 OVERVIEW

The focus of the current paper is to find errors caused by the fusion method used. Fusion errors occur when (i) two sensors’ outputs differ significantly, and then (ii) the logic of fusion (i.e., merging the sensor outputs) prioritizes the faulty outputs. To simulate such errors, *FusED* first efficiently searches (a.k.a. fuzz) the given driving environment to find scenarios that maximize the differences between the involved sensors and thus, lead to accidents (see Section 3.2). *FusED* then changes the existing fusion logic with alternative ones and check whether the updated logic can avoid the simulated crashes (see Section 3.3). If a collision is avoidable with alternative fusion logic, *FusED* concludes that original fusion logic was erroneous. Finally, *FusED* reports the unique fusion errors, as described in Section 3.4. This section summarizes these steps.

3.1 Defining Fusion Errors

Our goal is to simulate errors, i.e., accidents, that may happen due to incorrect fusion logic. A fusion error should have the following two properties:

- *Crash-inducing*: A simulation should witness a *crash* of the ego car. Since only the longitudinal control module in OPENPILOT uses fusion, we don’t consider the accidents likely caused by the misbehaviors of the latitudinal control. For example, we ignore scenarios in which OPENPILOT drives out of its current lane.
- *Fusion-induced*: The collision should be caused by the misbehavior of the fusion component. If the rest of the ADAS system and environment behave as it is, and we had a correct implementation of sensor fusion, the collision would not be observed.

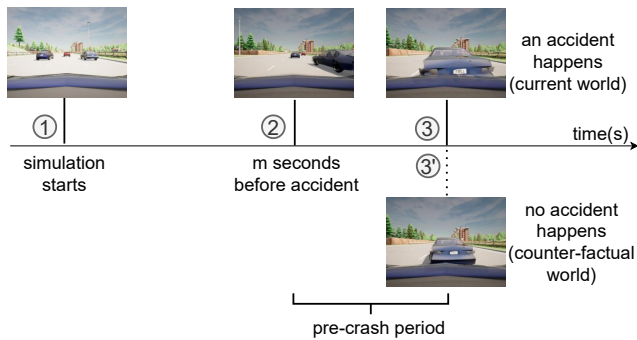


Figure 5: An illustration of pre-crash period and fusion error.

Figure 5 illustrates such a fusion error. At time ①, a simulation starts and OPENPILOT is engaged. The simulation enters the pre-crash period (i.e., the m seconds before an accident during which it starts to misbehave) at time ② and finally, a collision happens at ③. If a better fusion method is used from time ② onward, in the counter-factual world, no collision happens (at time ③).

3.2 Simulating Collisions with Fusion Fuzzing

To simulate fusion errors efficiently, we apply an evolutionary-based fuzzing algorithm that searches for the scenarios in which fusion errors are likely to happen. Since fusion errors have two properties: critical and fusion-induced (Section 3.1), we design the objective functions accordingly that our fuzzing aims to optimize.

For capturing *critical* (i.e., crash-inducing) property, we adopt the safety potential objective used in [31]. It represents the distance between the ego car and the leading vehicle (subtracted by the ego car’s minimum stopping distance)—minimizing it will facilitate the collision. We denote it as $F_{\text{dist}}(x)$ for the scenario x . To further promote collision, we introduce another boolean objective function (F_{error}) that is true only if a collision happens.

For the *fusion-induced* property, we want to increase the time during which the fusion method makes an inaccurate prediction while it has received an accurate prediction from at least one sensor. To achieve this, we maximize the number of time steps such that at each time step the fusion’s output is far from the ground-truth and at least one sensor output is close to the ground-truth. Given that we use a simulated environment for testing, we can easily get the ground-truth lead information from the simulator. We denote this objective as F_{fusion} and presents its details in Appendix B. Putting the above objectives together, we obtain the following fitness function that our evolutionary fuzzer tries to optimize (here c_i s are constants and can be set experimentally):

$$F(x) = c_{\text{error}}F_{\text{error}}(x) + c_dF_d(x) + c_{\text{fusion}}F_{\text{fusion}}(x) \quad (1)$$

3.3 Analyzing Root Causes of the Collisions

We next analyze the simulated errors reported in previous step and check they are indeed *caused* by the incorrect fusion logic. The most intuitive approach to check this would be to simply replace the fusion method with another fusion method and check if the collision still happens. However, this approach has two issues. First, compared with the initial simulation, some unobserved influential factors (e.g., non-determinism in sensor inputs, the communication delay between the simulator and OPENPILOT) might have changed. As a result, even if a collision does not occur with an alternative fusion logic, it might be due to the influence of other unobserved influential factors. Second, the alternative fusion logic chosen randomly may not be able to avoid the collision. Since simulation is costly, it is not possible to explore all the different logic (e.g., all the if-else branches in the fusion logic implementation Figure 3-a). Thus, we must choose the alternative fusion method carefully.

To address the first issue, we resort to the theory of causal analysis. In particular, we consider the fusion method used as the interested variable and the occurrence of a collision as the interested event. We then consider all other factors that can directly or indirectly influence the collision as well as their interactions based on domain knowledge. The goal is to control all the factors that influence the collision and are not influenced by the fusion method to stay same across the simulations. For those influential variables that cannot be controlled directly, we apply interventions on other variables such that the uncontrollable variable’s influence on the collision is eliminated. For example, to eliminate the influence of the communication latency, we set the communication configurations for OPENPILOT and simulator to be synchronous and deterministic.

Given the assumption that all the influential variables are controlled, if the collision is avoided after the replacement in a counterfactual world, we can say the fusion method used is the actual cause.

To address the second issue, we define a fusion method called *best-sensor fusion*, which always selects the sensor prediction that is closest to the ground-truth. This fusion method provides the best prediction among the sensors. Consequently, it is reasonable to assume that it should help to avoid the collision if the collision was due to the fusion method used.

3.4 Counting Fusion Errors

We design the principles for counting distinct fusion errors in this section. Note that error counting in simulation-based testing remains an open challenge. Related works [2, 34] consider two errors being different if the scenarios are different. This definition tends to over-count similar errors when the search space is high-dimensional. Another approach manually judges errors with human efforts [31]. Such way is subjective and time-consuming when the number of errors grows up.

Inspired by the location trajectory coverage metric [23], we consider the ego car's state (i.e., location and speed) during the simulation rather than the input space variables or human judgement. We split the pieces of the lane that ego car drives on into s intervals and the ego car's allowed speed range into l intervals to get a two-dimensional coverage plane with dimensions $1^{s \times l}$. During the simulation, the ego car's real-time location and speed are recorded. The recorded location-speed data points are then mapped to their corresponding "bins" on the coverage plane. Given all the data points mapped into the bins having the same road interval, their average speed is taken, the corresponding speed-road bin is considered "covered", and the corresponding field on the coverage plane is set 1. Note a simulation's final trajectory representation can have at most s non-zero fields.

We denote the trajectory vector associated with the simulation run for a specification x to be $\mathbf{R}(x)$ and define:

Definition 1. Two fusion errors for the simulations runs on specifications x_1 and x_2 are considered distinct if $\|\mathbf{R}(x_1) - \mathbf{R}(x_2)\|_0 > 0$.

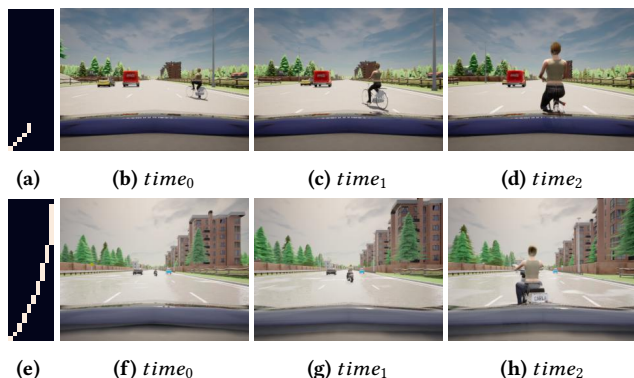


Figure 6: Examples of two fusion errors with different trajectories. (a) and (e) show speed-location coverage where the x-axis is speed and y axis is the road interval.

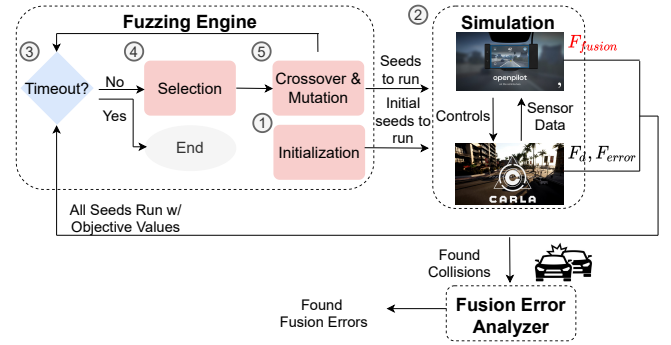


Figure 7: The overall workflow of FusED.

To demonstrate this error counting approach, we show two fusion errors with different trajectories in Figure 6. In both Figure 4 and the first row of Figure 6, the ego car hits a bicyclist cutting in from the right lane. The difference is only that the yellow car on the left lane has different behaviors across the two runs. However, the yellow car does not influence the ego car's behavior. Hence, the two simulation runs have the same trajectory coverage (ref. Figure 6a). By contrast, the other fusion error on the second row of Figure 6 has a different trajectory (ref. Figure 6e) that the ego car in high speed collides with a motorcycle at a location close to the destination. This example illustrates the necessity of counting fusion errors upon Definition 1.

4 FUSED METHODOLOGY

In this section, we introduce *FusED*, our automated framework for fusion errors detection. Figure 7 shows high-level workflow of *FusED*. It consists of three major components: the fuzzing engine, the simulation, and the fusion error analyzer. The fuzzer runs for predefined rounds of generations. At each generation, it feeds generated scenarios (a.k.a. *seeds*) into the simulation. In a simulation, at each time step, the CARLA simulator supplies the sensor data of the current scene to OPENPILOT. After OPENPILOT sends back its control commands, the scene in CARLA updates. After the simulations for all the seeds at the current generation have been run, the seeds along with their objective values in the simulations are returned as feedback to the fuzzer. Besides, all the collision scenarios are recorded. The fuzzer then leverages the feedback to generate new seeds in the execution of the next generation. After the fuzzing process ends, all the collision scenarios are rerun with the best-sensor fusion in the counterfactual world. The scenarios that avoid the collision are reported as fusion errors.

4.1 Fuzzing Algorithm

FusED aims at maximizing the number of found fusion errors within a given time budget. The search space is high-dimensional and the simulation execution is costly. Evolutionary-based search algorithms have been shown effective in such situation [31, 50]. We adopt an evolutionary-based search algorithm with a domain-specific fitness function (defined in Section 3.2) promoting fusion errors finding. We denote our method as *GA-FUSION*.

The fuzzer tries to minimize a fitness function over generations. At the beginning, random seeds are sampled from the search space and fed into the simulation, as shown by ① in Figure 7. In ②,

the simulation then runs OPENPILOT in CARLA with the supplied scenarios. The violations found are recorded and the seeds with the objective values are returned to the fuzzer accordingly. If the whole execution runs timeout, the fuzzing procedure ends (3). Otherwise, seeds are ranked based on their objective values for further *selection* (4). The fuzzer performs *crossover and mutation* operations among the selected seeds to generate new seeds (5) for the simulation. The steps (2)-(5) repeat until reaching the time threshold. The details for each step can be found in Appendix B.

4.2 Root Cause Analysis

This step analyzes the fusion errors found by the fuzzer to confirm the incorrect fusion logic causes them. As described in Section 3.3, we leverage causal analysis to find the root cause of the errors, and if fusion logic is not the reason behind an error, we filter it out.

Problem Formulation. In causality analysis, the world is described by variables in the system and their causal dependencies. Some variables may have a causal influence on others. This can be represented by a Graphical Model [39], as shown in Figure 8, where the graph nodes represent the variables, and the edges connect the nodes that are causally linked with each other. For example, the test scenario should influence the occurrence of a collision. In a scenario involving many NPC vehicles, OPENPILOT is more likely to misbehave. The variables are typically split into two sets: *the exogenous variables (U)*, whose values are determined by factors outside the model, and *the endogenous variables (V)*, whose values are ultimately determined by the exogenous variables.

In our context, we define \vec{X} to be the fusion method, \vec{Y} to be a boolean variable representing the occurrence of a collision, and $\phi = \vec{Y}$. \vec{Z} is the union of \vec{X} and \vec{Y} . \vec{W} is the complement of \vec{Z} in V . Since we know a collision (ϕ holds) happens when a fusion method is used ($\vec{X} = \vec{x}$), following the actual cause of [21], the fusion method is an actual cause of the collision if: when another fusion method is used ($\vec{X} = \vec{x}'$), and all other endogenous variables (which influence the collision and are not influenced by the fusion method) are kept the same as in the original collision scenario ($\vec{W} = \vec{w}$), the collision can be avoided. The details can be found in Appendix A.

Simulation Causal Relations Analysis In order to check if a fusion error satisfies this definition, we construct a causal graph (Figure 8) specifying the relevant variables based on domain knowledge. We also make an assumption that all the variables potentially influencing the occurrence of a collision have been included in the graph. The exogenous variables include test design and the state of the system running simulation (e.g., real-time CPU workload, memory usage, etc.). Test design determines scenario to test, simulator configurations, and OPENPILOT configurations (including the fusion method). Another endogenous variable "communication latency" collectively represents the real-time latency of the communications between the simulator and OPENPILOT as well as among each of their sub-components. This variable captures the uncertainty caused by the state of the system running the simulation. It is influenced by the communication configurations of simulator and OPENPILOT, as well as the system state. In a system with limited CPU capacity available, the latency can become very high and

results in the delay of the sensor information passed from the simulator to OPENPILOT. Consequently, collision might be more likely to happen. Finally, scenario, simulator configurations, OPENPILOT configurations, and the communication latency jointly influence the occurrence of a collision in the simulation.

To check for causality, we need to be able to control the endogenous variables \vec{W} and block any influence of the unobserved exogenous variables on the collision. However, we cannot control the communication latency since one of its parents – the system state variable cannot be observed and controlled. To address it, we set the communication configurations of the simulator and the OPENPILOT to be deterministic and synchronous (see Appendix D for details). The communication latency then becomes 0 and can be ignored. Note such change is kept throughout the entire fuzzing process. Further, during the fusion error analyzing step, we replace the initial fusion method (\vec{x}) with another fusion method (\vec{x}') and check if a collision still happens. This step is regarded as an intervention on the fuzzing method after the fuzzing process.

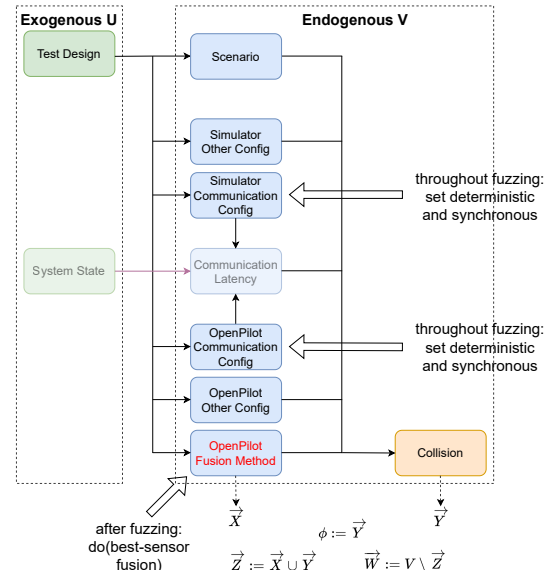


Figure 8: Illustrating the causal graph with intervention.
Fusion Replacement Analysis The next step is to efficiently find a fusion method x' avoiding collision. The fusion method x' should possess additional properties like being realistic and functional. Being realistic means that it should not have extra knowledge (e.g., the ground-truth of the locations of the NPC vehicles) beyond what it receives from the upstream sensor modules. Being functional means it should be good enough to enable the ego car to finish the original task. A counter-example is if the fusion method always false positively report the presence of a stationary NPC vehicle ahead and leads the ego car to stay stationary all the time. Collision can be avoided in this case since the ego car does not move at all but the original task is not completed neither.

To illustrate this, we define three different classes of fusion methods. Given everything else is kept the same, *collision fusion class* and *non-collision fusion class* consist of the fusion methods that lead to and avoid the collision, respectively. *Realistic & functional class*

consists of fusion methods which are both realistic and functional. If an error is caused by the fusion method and can be fixed by changing it to a realistic and functional fusion method, there should be an intersection between non-collision fusion and realistic & functional fusion as shown in Figure 9(a) and Figure 9(c). Otherwise, there should be no intersection between the two and the realistic & functional fusion class should be a subset of the collision fusion class as shown Figure 9(b). The initial fusion method should fall into the intersection of the collision fusion class and the realistic & functional fusion class since a collision happens and it is reasonable to assume it (DEFAULT or MATHWORKS) is realistic and functional.

In the current work, for each found collision, we only run one extra simulation to check if the fusion method is the cause. In particular, we set \vec{x}' to *best-sensor fusion*. Note that this fusion method is an oracle fusion method since in reality we won't be able to know the ground-truth. However, it serves a good proxy. First, it is realistic. Although it uses ground-truth, in reality, a fusion method might potentially achieve the best-sensor fusion method's output which is the most reliable upstream sensor's prediction. Second, it is functional since it provides more accurate prediction than methods like DEFAULT and thus should be able to finish the original cruising task. Third, if *best-sensor fusion* cannot help to avoid a collision after the replacement, there is a high possibility that the collision is not due to the fusion method. The reason is that it already picks the best sensor prediction and it is reasonable to assume that the downstream modules are more likely to perform better given its output compared with those less accurate outputs.

Thus, best-sensor fusion serves as a proxy to check if there is an intersection between realistic & functional fusion and non-collision fusion. If best-sensor fusion can help avoid the collision, the error will be considered a fusion error. Otherwise, it will be discarded. There are three situations: (a) the error is caused by the fusion method and the best-sensor fusion falls into non-collision fusion class (Figure 9a). (b) the error is not caused by the fusion method and the best-sensor fusion does not fall into non-collision fusion class (Figure 9b). (c) the error is caused by the fusion method and the best-sensor fusion does not fall into non-collision fusion class (Figure 9c). (a) and (b) are the true positive and true negative cases since the causation of the fusion method is consistent with the collision results of the best-sensor fusion method, while (c) is the false negative case. It also should be noted that there is no false positive case since if best-sensor fusion helps avoiding the collision, according to our reasoning earlier, the causation must hold. The implication is that a fusion error is an error caused by the fusion method but the reverse does not always hold.

5 RESULTS

To evaluate *FusED*, we explore the following research questions:

RQ1: Evaluating Performance. How effectively can *FusED* find fusion errors in comparison to baselines?

RQ2: Case Study of Fusion Errors. What are the representative causes of the fusion errors found?

RQ3: Evaluating Repair Impact. How to improve Multi-Sensor Fusion in OPENPILOT based on our observations on found fusion errors?

5.1 Experimental Design

Environment. We use CARLA 0.9.11 [17] as the simulator and OPENPILOT 0.8.5 as the ADAS [15]. The experiments run on a Ubuntu20.04 desktop with Intel i9-7940x, Nvidia 2080Ti, and 32GB memory.

Studied Fusion Methods. We apply *FusED* on DEFAULT and MATHWORKS introduced in Section 2.2.

Driving Environments. We utilize two driving environments named S1 and S2 in our study. S1 is a straight local road and S2 is a left curved highway road. An illustration is shown in Figure 10 (not all NPC vehicles are shown). Both S1 and S2 have 6 NPC vehicles. The maximum allowed speed of the auto-driving car is set to 45 miles/hr on the highway road (S2) and 35 miles/hr on the local road (S1). For vehicle types, S2 only considers cars and trucks while S1 additionally includes motorcycles and bicyclists. The search space for each vehicle consists of its type, its speed (from 0 to 150% of the maximum allowed speed of the current road) and lane change decision (turn left/right, or stay in lane) at each time interval. Weather and lighting conditions are also searchable. In total, The search space consists of 76 dimensions (see Appendix F for details).

Baselines and Metrics. We use random search (RANDOM) and genetic algorithm without F_{fusion} in the fitness function (GA) as two baselines. We set the number of scenarios causing fusion errors and distinct fusion errors (Definition 1) as two evaluation metrics.

Hyper-parameters. We set the default values for c_{error} , c_d , c_{fusion} in the fitness function to be $-1, 1, -2$. Since the crash-inducing property has two terms (c_{error} and c_d) while the fusion aspect only has one (c_{fusion}), the choice of these default values balances the contribution of the two. The sign for c_d is positive since we want to minimize F_d and the signs for the other two are negative since we want to maximize F_{error} and F_{fusion} . We set the pre-crash period's m to 2.5 seconds because several states in US use 2.5s as the standard driver reaction time and studies have found the 95 percentile of perception-reaction time for human drivers is 2.5s [30]. Besides, in our context, when a fusion-induced collision happens, it is often caused by the fusion component's failure for about 2.5s before the collision as in Figure 4. We set s and l (defined in Section 3.4) to 30 and 10 such that each road interval is about 5m and each speed interval is about 4m/s. By default, we fuzz for 10 generations with 50 simulations per generation; each simulation runs at most 20 simulation seconds.

5.2 RQ1: Evaluating Performance

We compare GA-FUSION with the two baselines. Figure 11 shows the average number of fusion errors found by the three methods over three runs for each setting. On average GA-FUSION has found 65%, 27%, 23%, 44% more fusion errors than the best baseline method under each setting, respectively. Figure 12 shows the average number of distinct fusion errors (based on Definition 1) found by the three methods over three runs for each setting. GA-FUSION has also found 58%, 31%, 25%, and 37% more distinct fusion errors than the best baseline method, respectively.

To test the significance of the results, we further conduct Wilcoxon rank-sum test [12] and Vargha-Delaney effect size test [8, 45] between the number of distinct fusion errors found by GA-FUSION and the best baseline under each setting. For each of the four settings, we have the p-value 0.05 and VD effect size interval (0.68, 1.32) at

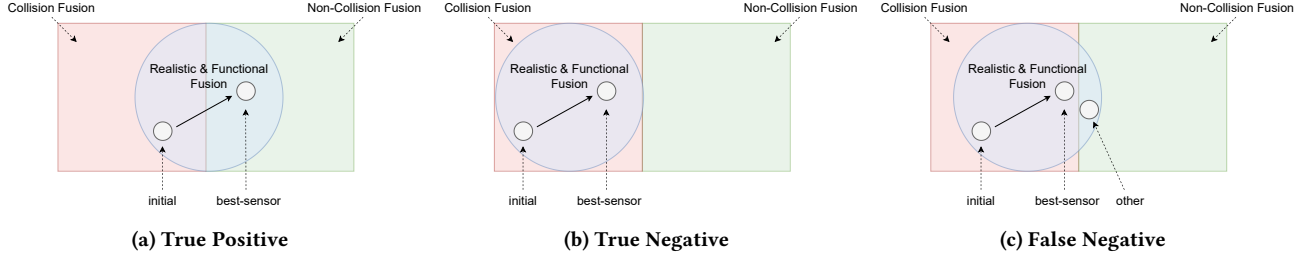


Figure 9: An illustration of three situations of replacing the fusion method.

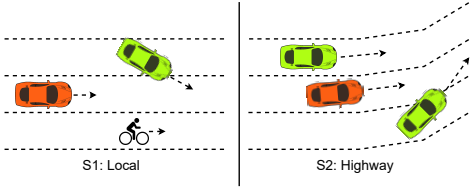


Figure 10: An illustration of the two driving environments where the orange car represents the ego car.

the 90% confidence interval, suggesting the difference is significant and the difference has medium effect size. These results show the effectiveness of *FusED* and superiority of *GA-FUSION*.

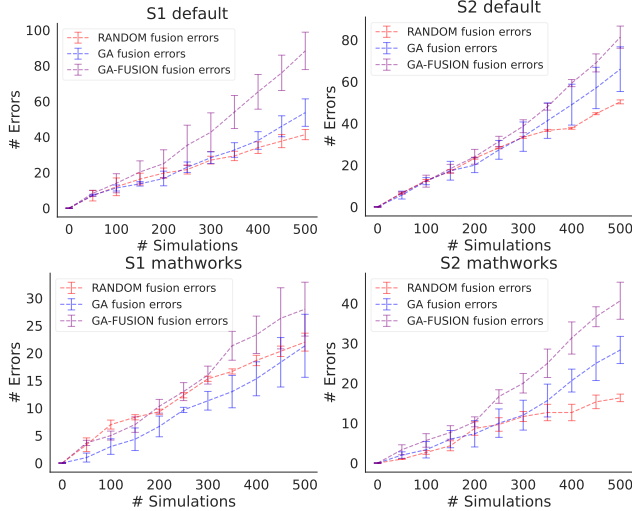


Figure 11: # fusion errors found over # simulations.

The reason the proposed *GA-FUSION* can find more fusion errors is that our proposed F_{fusion} can differentiate fusion errors from non-fusion errors. Figure 13 shows the distribution density of F_{fusion} of normal (i.e. no collision happens), non-fusion errors, and fusion errors when running *GA-FUSION* under the four settings. In Figure 13a, Figure 13c, and Figure 13d, fusion errors have much larger F_{fusion} than non-fusion errors. The Cohen's d effect size test [41] between them are 2.06, 1.08, 1.43, respectively, and the Wilcoxon rank-sum test has the p-value $1.8e^{-13}$, $5.5e^{-4}$, $5.1e^{-5}$, respectively, suggesting large difference with significance for all three. In Figure 13b, fusion errors also show larger F_{fusion} than non-fusion errors. The Cohen's d effect size test [41] between them is 0.72 and the Wilcoxon

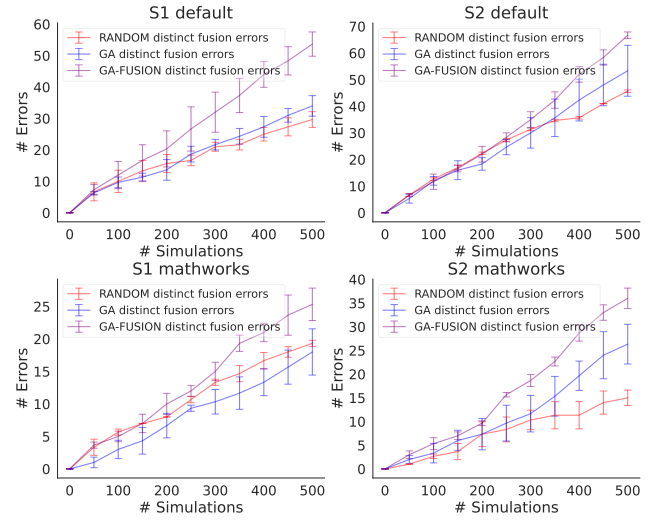
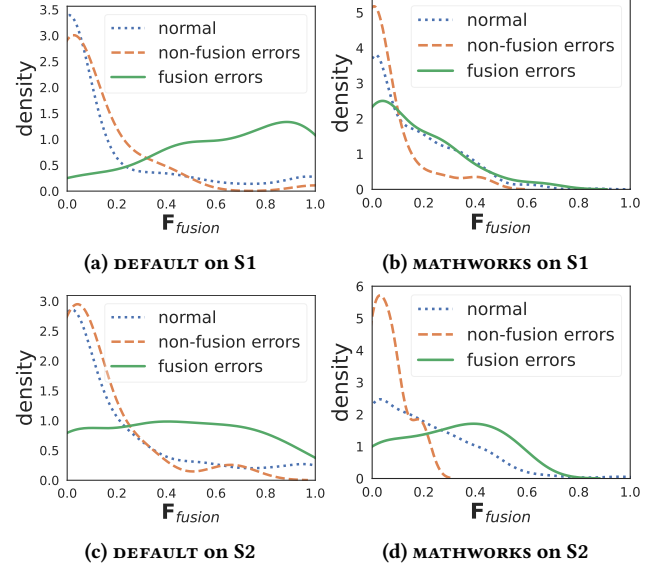


Figure 12: # distinct fusion errors found over # simulations.

Figure 13: Distribution density of F_{fusion} .

rank-sum test has the p-value $8.1e^{-3}$, meaning a medium difference with significance. Overall, the difference between fusion errors and

non-fusion errors with respect to F_{fusion} shows the effectiveness of F_{fusion} and thus the gain of GA-FUSION.

Result 1: *On average, FusED finds 25%-58% more distinct fusion errors over the best baseline method under the four settings.*

5.3 RQ2: Case Study of Fusion Errors.

In this subsection, we show three representative fusion errors found by *FusED* and analyze their root causes.

Case1: Incorrect camera lead dominates accurate radar lead. The first row of Figure 14 shows a failure due to the misbehavior of ② in Figure 3a. In Figure 14a, both camera and radar give accurate prediction of the leading green car at $time_0$. At $time_1$ in Figure 14b, the green car tries to change lane, collides with a red car, and blocks the road. The camera model predicts that the green car with a low confidence (49.9%) and the fusion component thus misses all leading vehicles due to ② in Figure 3a. The ego car keeps driving until hitting the green car at $time_2$ in Figure 14c. If the radar data is used instead from $time_0$, however, the accident can be avoided, as shown in Figure 14d. Going back to Figure 3a, the root cause is that OPENPILOT prioritizes the camera prediction and it ignores any leading vehicles if the camera prediction confidence is below 50%. As a result, despite the accurate information predicted by the radar, OPENPILOT still causes the collision.

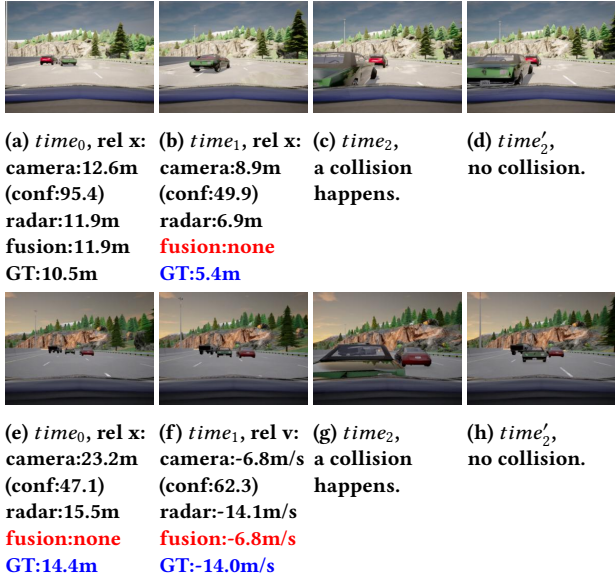


Figure 14: Two found fusion errors for **DEFAULT**. $rel\ v$ represents relative speed to the leading NPC vehicle.

Case2: Inaccurate radar lead selected due to mismatch between radar and camera. The second row of Figure 14 shows another failure caused by both ② and ③ in Figure 3a. At $time_0$ of Figure 14e, camera overestimates the longitudinal distance to the leading green car. At $time_1$ of Figure 14f, though one radar data (not shown) is close to the correct information of the green car, the radar data of the Cybertruck on the left lane matches the camera's prediction. Thus, the Cybertruck lead data is selected regarding

③ in Figure 3a. Consequently, although the ego car slows down, the process takes longer time than if it selects the green car radar data. This finally results in the collision at $time_2$ in Figure 14g. If the green car radar lead is used from $time_0$, the ego car would slow down quickly and thus not hit the green car at $time_2'$ in Figure 14h. This failure also correlates to camera dominance but it additionally involves mismatching in ③ of Figure 3a.

Case3: Discarding correct lead due to a faulty selection method.

Figure 15 shows an example when MATHWORKS fails due to ③ in Figure 3b. At $time_0$ in Figure 15a, a police car on the right lane is cutting in. While radar gives a very accurate prediction of the red car, the radar prediction is not used since ③ in Figure 3b only selects among the predicted leads within the current lane. Consequently, a camera predicted lead is used, which overestimates the relative longitudinal distance. At $time_1$ in Figure 15b, the correct radar prediction is used but it is too late for the ego car to slow down, causing the collision at $time_2$ in Figure 15c. If the best predicted lead (i.e. the one from the radar data) is used starting at $time_0$, the collision would disappear at the time $time_2'$ of Figure 15d.



Figure 15: A found fusion error for **MATHWORKS**.

Result 2: *The representative fusion errors found by FusED for the two fusion methods are due to the dominance of camera over radar, their mismatch, or the faulty selection method of the prediction.*

5.4 RQ3: Evaluating Repair Impact.

To avoid the fusion errors, one obvious alternative to the studied fusion methods seems to simply let the radar predictions dominate the camera predictions as the examples shown in Section 5.3 are mainly caused by the dominance of unreliable camera prediction. Such design, however, suffers from how to choose the fusion leads from all radar predicted leads. If the fusion method simply chooses the closest radar lead and that lead corresponds to an NPC vehicle on a neighboring lane, the ego car may never pass the NPC vehicle longitudinally even when the NPC vehicle drives at a low speed.

Based on our observation and analysis of the above fusion errors, we suggest two improvements to enhance the fusion methods. First, radar predictions should be integrated rather than dominated by camera predictions (Cases 1-2). Second, vehicles intending to cut in should be tracked and considered (Case 3). MATHWORKS already addresses the first aspect and thus has less fusion errors found. Regarding the second one, for each tracked object by radar, we store their latitudinal positions at each time step. At next time step,

if a vehicle’s relative latitudinal position gets closer to the ego car, it will be included in the candidate pool for the leading vehicle rather than discarded. We call this new fusion method **MATHWORKS+**.

S1 DEFAULT	S1 MATHWORKS	S2 DEFAULT	S2 MATHWORKS
43/52	14/26	67/78	13/26

Table 1: # avoided / # distinct fusion errors.

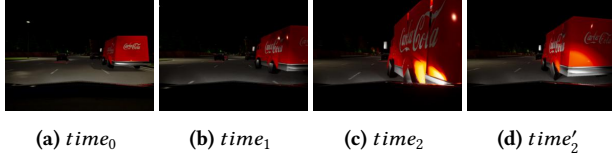


Figure 16: An fusion error avoided by **MATHWORKS+**.

We evaluate **MATHWORKS+** by replacing the original fusion method with it during the pre-crash window on the previously found fusion errors. As shown in Section 5.4, at least 50% of found fusion errors can be avoided. Figure 16 shows a fusion error found on **MATHWORKS** but avoided by **MATHWORKS+**. At $time_0$ (Figure 16a), the ego car and a red truck drive on different lanes. At $time_1$, **MATHWORKS** does not consider the truck since it just starts to invade into the current lane (the truck’s radar lead is discarded at ③ in Figure 3b). When the truck fully drives into the current lane, it is too late for the ego car to avoid the collision at $time_2$ (Figure 16c). If **MATHWORKS+** is used since Figure 16a, the truck would be considered a leading vehicle at Figure 16b and the collision would be avoided at $time'_2$ (Figure 16d). These results demonstrate the improvement of **MATHWORKS+**. Further, it implies that with a good fusion method, many fusion errors can be avoided without modifying the sensors or the processing units.

Result 3: *Based on the observations of the found fusion errors, we adjust the fusion method we study and enable it to avoid more than 50% of the initial fusion errors.*

6 RELATED WORK

Scenario-Based Testing. In order to identify the errors of a driving automation system, comprehensive tests are being conducted by autonomous driving companies. The public road testing approach is the closest to a system’s use case, but it is incredibly costly. It has been shown that more than 11 billion miles are required to have a 95% confidence that a system is 20% safer than an average human driver[26]. Most of these miles, however, usually do not pose threats to the system under test and are thus not efficient, if not wasted. To focus on interesting test cases, scenario-based testing techniques have been developed where a system is tested in some difficult scenarios either designed by experts or searched by algorithms. Besides, since many dangerous cases (e.g., a pedestrian crossing a street close to the ego car) cannot be tested in the real world, such tests are usually conducted in a high-fidelity simulator. Existing works usually treat the system under test as a black-box and search for hard scenarios to trigger ego car’s potential misbehaviors [2, 5, 10, 14, 16, 19, 20, 23, 27–29, 31, 38, 46, 47, 50, 51].

The errors found can have different causes like the failure of the sensors, the issue of the planning module, or some interactions among the modules. However, most existing works either ignore the root cause analysis or merely analyze causes for general errors. In contrast, we focus on revealing errors causally induced by the fusion component. Similar to the current work, Abdessalem et al. [3] study the interaction failure of several components in an ADAS. However, we focus on the fusion component which integrates the data from multiple sensor processing modules while they study the integration module which integrates the decisions of different functionalities (e.g., AEB and ACC). Besides, the fusion component can either be rule-based (e.g., **DEFAULT**) or algorithm-based (e.g., **MATHWORKS**) while the integration component studied in [3] is only rule-based.

Adversarial Attacks on Fusion. Some recent works study how to attack the fusion component of an automated system and thus fails the system [11, 42, 44]. In particular, Cao et al.[11] and Tu et al.[44] study how to construct adversarial objects that can fool both camera and Lidar at the same time and thus lead the MSF to fail. Shen et al.[42] study how to send spoofing GPS signals to confuse a MSF on GPS and Lidar. In contrast to creating artificial adversarial objects or sending adversarial signals, we focus on finding scenarios under which the failure of MSF leads to critical accidents without the presence of any malicious attacker.

7 THREATS TO VALIDITY

There remains a gap between testing in real-world and testing in a simulator. However, road testing is overly expensive and not flexible. Besides, a simulation environment allows us to run counterfactual simulations easily and attribute an error to the fusion method used. Consequently, we focus on testing in the simulation environment.

As in previous works [2, 34], we evaluate the proposed method using the number of found scenarios leading to fusion errors. However, we have observed that this metric might double counts similar fusion errors. To mitigate this threat, we additionally use another counting metric based on the ego car’s trajectory (Section 3.4). A more fine-grained metric can be developed by considering the inputs and outputs of the fusion component. We leave its exploration for future work.

Besides, similar to previous works[2, 31], we evaluate the studied ADAS on two driving environments. Since ADAS only performs the task of lane following, the complexity of its applicable environments is limited. The two environments we consider has covered most of its applicable road situations.

Another threat is that the hyper-parameters (e.g., the coefficients of the search objective) are not fully fine-tuned. However, even with the current parameters, the proposed method already outperforms the baselines. We believe that the performance of the proposed method can be further improved by fine-tuning the hyper-parameters.

Furthermore, we only test **MATHWORKS+** on limited detected fusion errors on OPENPILOT. There might be corner cases that are not covered. Since we focus on fusion errors finding rather than fixing, we leave a comprehensive study for future work.

Finally, the current fusion objective only applies to HLF and is only tested on two popular fusion methods in OPENPILOT. Conceptually, the proposed method can generalize to the fusion component in ADS like Apollo[9] and Autoware[43] which use HLF components. We plan to study other types of fusion methods like MLF and LLF, as well as MSF in ADS in future work.

8 CONCLUSION

In this work, we formally define, expose, and analyze the root causes of fusion errors on two widely used MSF methods in a commercial ADAS. To the best of our knowledge, our work is the first study on finding and analyzing errors causally induced by MSF in an end-to-end system. We propose a grey-box fuzzing framework, *FusED*, that effectively detects fusion errors. Lastly, based on the analysis of the found fusion errors, we provide several learned suggestions on how to improve the studied fusion methods.

REFERENCES

[1] 2022. Tesla Deaths. <https://www.tesladeaths.com/>.

[2] Raja Ben Abdessalem, Shiva Nejati, Lionel C. Briand, and Thomas Stifter. 2018. Testing Vision-Based Control Systems Using Learnable Evolutionary Algorithms. In *Proceedings of the 40th International Conference on Software Engineering* (Gothenburg, Sweden) (ICSE '18). Association for Computing Machinery, New York, NY, USA, 1016–1026. <https://doi.org/10.1145/3180155.3180160>

[3] Raja Ben Abdessalem, Annibale Panichella, Shiva Nejati, Lionel C. Briand, and Thomas Stifter. 2018. Testing Autonomous Cars for Feature Interaction Failures Using Many-Objective Search. In *Proceedings of the 33rd ACM/IEEE International Conference on Automated Software Engineering* (Montpellier, France) (ASE 2018). Association for Computing Machinery, New York, NY, USA, 143–154. <https://doi.org/10.1145/3238147.3238192>

[4] Raja Ben Abdessalem, Annibale Panichella, Shiva Nejati, Lionel C. Briand, and Thomas Stifter. 2020. Automated Repair of Feature Interaction Failures in Automated Driving Systems. In *Proceedings of the 29th ACM SIGSOFT International Symposium on Software Testing and Analysis* (Virtual Event, USA) (ISSTA 2020). Association for Computing Machinery, New York, NY, USA, 88–100. <https://doi.org/10.1145/3395363.3397386>

[5] Y. Abeyisirigoonawardena, F. Shkurti, and G. Dudek. 2019. Generating Adversarial Driving Scenarios in High-Fidelity Simulators. In *2019 International Conference on Robotics and Automation* (ICRA). 8271–8277.

[6] National Highway Traffic Safety Administration. 2020. Common Driver Assistance Technologies. (2020). <https://www.safercar.gov/equipment/driver-assistance-technologies>

[7] Ram Agrawal, Kalyanmoy Deb, and Ram Agrawal. 2000. Simulated Binary Crossover for Continuous Search Space. *Complex Systems* 9 (06 2000).

[8] Andrea Arcuri and Lionel Briand. 2014. A Hitchhiker’s guide to statistical tests for assessing randomized algorithms in software engineering. *Software Testing, Verification and Reliability* 24, 3 (2014), 219–250. <https://doi.org/10.1002/stvr.1486>

[9] BaiduApolloTeam. 2021. Apollo: Open Source Autonomous Driving. <https://github.com/ApolloAuto/apollo>. Accessed: 2019-02-11.

[10] R. Ben Abdessalem, S. Nejati, L. C. Briand, and T. Stifter. 2016. Testing advanced driver assistance systems using multi-objective search and neural networks. In *2016 31st IEEE/ACM International Conference on Automated Software Engineering* (ASE). 63–74.

[11] Yulong Cao, Ningfei Wang, Chaowei Xiao, Dawei Yang, Jin Fang, Ruigang Yang, Q. Chen, Mingyan D. Liu, and Bo Li. 2021. Invisible for both Camera and LiDAR: Security of Multi-Sensor Fusion based Perception in Autonomous Driving Under Physical-World Attacks. *ArXiv* abs/2106.09249 (2021).

[12] J. Anthony Capon. 1991. Elementary Statistics for the Social Sciences: Study Guide. (1991).

[13] Aditya Chattopadhyay, Piyushi Manupriya, Anirban Sarkar, and Vineeth N Balasubramanian. 2019. Neural Network Attributions: A Causal Perspective. In *Proceedings of the 36th International Conference on Machine Learning* (Proceedings of Machine Learning Research, Vol. 97), Kamalika Chaudhuri and Ruslan Salakhutdinov (Eds.). PMLR, 981–990. <https://proceedings.mlr.press/v97/chattopadhyay19a.html>

[14] Baiming Chen and Liang Li. 2020. Adversarial Evaluation of Autonomous Vehicles in Lane-Change Scenarios.

[15] CommaAI. 2021. Openpilot. <https://github.com/commaai/openpilot>

[16] Wenhao Ding, Baiming Chen, Minjun Xu, and Ding Zhao. 2020. Learning to Collide: An Adaptive Safety-Critical Scenarios Generating Method. In *IEEE/RSJ International Conference on Intelligent Robots and Systems (IROS)* (Virtual). <https://arxiv.org/abs/2003.01197>

[17] Alexey Dosovitskiy, German Ros, Felipe Codevilla, Antonio Lopez, and Vladlen Koltun. 2017. CARLA: An Open Urban Driving Simulator (*Proceedings of Machine Learning Research*, Vol. 78), Sergey Levine, Vincent Vanhoucke, and Ken Goldberg (Eds.). PMLR, 1–16. <http://proceedings.mlr.press/v78/dosovitskiy17a.html>

[18] Martin Ester, Hans-Peter Kriegel, Jörg Sander, and Xiaowei Xu. 1996. A Density-Based Algorithm for Discovering Clusters in Large Spatial Databases with Noise. In *Proceedings of the Second International Conference on Knowledge Discovery and Data Mining* (Portland, Oregon) (KDD’96). AAAI Press, 226–231.

[19] Hermann Felbinger, Florian Klück, Yihao Li, Mihai Nica, Jianbo Tao, Franz Wotawa, and Martin Zimmermann. 2019. Comparing two systematic approaches for testing automated driving functions. In *2019 IEEE International Conference on Connected Vehicles and Expo (ICCVE)*. 1–6. <https://doi.org/10.1109/ICCVE45908.2019.8965209>

[20] Alessio Gambi, Marc Mueller, and Gordon Fraser. 2019. Automatically Testing Self-Driving Cars with Search-Based Procedural Content Generation. In *Proceedings of the 28th ACM SIGSOFT International Symposium on Software Testing and Analysis* (Beijing, China) (ISSTA 2019). Association for Computing Machinery, New York, NY, USA, 318–328. <https://doi.org/10.1145/3293882.3330566>

[21] Joseph Y. Halpern. 2015. A Modification of the Halpern-Pearl Definition of Causality. In *Proceedings of the 24th International Conference on Artificial Intelligence* (Buenos Aires, Argentina) (IJCAI’15). AAAI Press, 3022–3033.

[22] Michael Harradon, Jeff Druce, and Brian E. Ruttenberg. 2018. Causal Learning and Explanation of Deep Neural Networks via Autoencoded Activations. *CoRR* abs/1802.00541 (2018). arXiv:1802.00541 <http://arxiv.org/abs/1802.00541>

[23] Zhisheng Hu, Shengjian Guo, Zhenyu Zhong, and Kang Li. 2021. Coverage-based Scene Fuzzing for Virtual Autonomous Driving Testing. *arXiv* (2021).

[24] Consumer Reports Data Intelligence. 2020. Active Driving Assistance Systems: Test Results and Design Recommendations. <https:////data.consumerreports.org/wp-content/uploads/2020/11/consumer-reports-active-driving-assistance-systems-november-16-2020.pdf>

[25] SAE International. 2021. J3016 Taxonomy and Definitions for Terms Related to Driving Automation Systems for On-Road Motor Vehicles. (2021).

[26] Nidhi Kalra and Susan M. Paddock. 2016. *Driving to Safety: How Many Miles of Driving Would It Take to Demonstrate Autonomous Vehicle Reliability?* RAND Corporation. <http://www.jstor.org/stable/10.7249/j.ctt1btcoxw>

[27] Florian Klück, Martin Zimmermann, Franz Wotawa, and Mihai Nica. 2019. Performance Comparison of Two Search-Based Testing Strategies for ADAS System Validation. In *Testing Software and Systems*, Christophe Gaston, Nikolai Kosmatov, and Pascale Le Gall (Eds.). Springer International Publishing, Cham, 140–156.

[28] M. Koren, S. Alsaif, R. Lee, and M. J. Kochenderfer. 2018. Adaptive Stress Testing for Autonomous Vehicles. In *2018 IEEE Intelligent Vehicles Symposium (IV)*. 1–7. <https://doi.org/10.1109/IVS.2018.8500400>

[29] Sampo Kuutti, Saber Fallah, and Richard Bowden. 2020. Training Adversarial Agents to Exploit Weaknesses in Deep Control Policies.

[30] Robert Layton and Karen Dixon. 2012. Stopping Sight Distance. (2012).

[31] Guanpeng Li, Yiran Li, Saurabh Jha, Timothy Tsai, Michael Sullivan, Siva Kumar Sastry Hari, Zbigniew Kalbarczyk, and Ravishankar Iyer. 2020. AV-FUZZER: Finding Safety Violations in Autonomous Driving Systems. In *2020 IEEE 31st International Symposium on Software Reliability Engineering (ISSRE)*. 25–36. <https://doi.org/10.1109/ISSRE5003.2020.00012>

[32] Yu Li, Devesh K. Jha, Asok Ray, and Thomas A. Wettergren. 2015. Feature level sensor fusion for target detection in dynamic environments. In *2015 American Control Conference (ACC)*. 2433–2438. <https://doi.org/10.1109/ACC.2015.7171097>

[33] Yuzhe Ma, Jon A. Sharp, Ruizhe Wang, Earlene Fernandes, and Xiaojin Zhu. 2021. Sequential Attacks on Kalman Filter-based Forward Collision Warning Systems. In *Thirty-Fifth AAAI Conference on Artificial Intelligence, AAAI 2021, Thirty-Third Conference on Innovative Applications of Artificial Intelligence, IAAI 2021, The Eleventh Symposium on Educational Advances in Artificial Intelligence, EAAI 2021, Virtual Event, February 2-9, 2021*. AAAI Press, 8865–8873. <https://ojs.aaai.org/index.php/AAAI/article/view/17073>

[34] R Majumdar, A Mathur, M Pirron, L Stegner, and D Zufferey. 2021. Paracosm: A Test Framework for Autonomous Driving Simulations. *Fundamental Approaches to Software Engineering* (2021).

[35] V. Manes, H. Han, C. Han, s. cha, M. Egele, E. J. Schwartz, and M. Woo. 2019. The Art, Science, and Engineering of Fuzzing: A Survey. *IEEE Transactions on Software Engineering* 01 (oct 2019), 1–1. <https://doi.org/10.1109/TSE.2019.2946563>

[36] Mathwork. 2021. Forward Collision Warning Using Sensor Fusion.

[37] Justin Norden, Matthew O’Kelly, and Aman Sinha. 2019. Efficient Black-box Assessment of Autonomous Vehicle Safety. In *Machine Learning for Autonomous Driving Workshop at the 33rd Conference on Neural Information Processing Systems (NeurIPS 2019)*.

[38] Matthew O’Kelly, Aman Sinha, Hongseok Namkoong, Russ Tedrake, and John C Duchi. 2018. Scalable End-to-End Autonomous Vehicle Testing via Rare-event Simulation. In *Advances in Neural Information Processing Systems*, S. Bengio, H. Wallach, H. Larochelle, K. Grauman, N. Cesa-Bianchi, and R. Garnett (Eds.), Vol. 31. Curran Associates, Inc., 9827–9838. <https://proceedings.neurips.cc/paper/>

2018/file/653c579e3f9ba5c03f2f2f8cf4512b39-Paper.pdf

[39] Judea Pearl. 1998. Graphical models for probabilistic and causal reasoning. *Quantified representation of uncertainty and imprecision* (1998), 367–389.

[40] Delphi Automotive PLC. 2019. Delphi Electronically Scanning RADAR. <https://hexagondownloads.blob.core.windows.net/public/AutonomouStuff/wp-content/uploads/2019/05/delphi-esr-whitelabel.pdf>

[41] S. Sawilowsky. 2009. New Effect Size Rules of Thumb. *Journal of Modern Applied Statistical Methods* 8 (2009), 26.

[42] Junjie Shen, Jun Won, Zeyuan Chen, and Qi Alfred Chen. 2020. Drift with Devil: Security of Multi-Sensor Fusion based Localization in High-Level Autonomous Driving under GPS Spoofing (Extended Version). In *USENIX Security Symposium 2020*.

[43] TheAutowareFoundation. 2016. Autoware: Open-source software for urban autonomous driving. <https://github.com/CPFL/Autoware>

[44] James Tu, Huichen Li, Xincheng Yan, Mengye Ren, Yun Chen, Ming Liang, Eilyan Bitar, Ersin Yumer, and Raquel Urtasun. 2021. Exploring Adversarial Robustness of Multi-Sensor Perception Systems in Self Driving. (01 2021).

[45] András Vargha and Harold D. Delaney. 2000. A Critique and Improvement of the CL Common Language Effect Size Statistics of McGraw and Wong. *Journal of Educational and Behavioral Statistics* 25, 2 (2000), 101–132. <https://doi.org/10.3102/10769986025002101> arXiv:<https://doi.org/10.3102/10769986025002101>

[46] Ding Wenhao, Chen Baiming, Li Bo, Ji Eun Kim, and Zhao Ding. 2020. Multimodal Safety-Critical Scenarios Generation for Decision-Making Algorithms Evaluation. In *arxiv*.

[47] T. A. Wheeler and M. J. Kochenderfer. 2019. Critical Factor Graph Situation Clusters for Accelerated Automotive Safety Validation. In *2019 IEEE Intelligent Vehicles Symposium (IV)*. 2133–2139. <https://doi.org/10.1109/IVS.2019.8813845>

[48] De Jong Yeong, Gustavo Velasco-Hernandez, John Barry, and Joseph Walsh. 2021. Sensor and Sensor Fusion Technology in Autonomous Vehicles: A Review. *Sensors* 21, 6 (2021). <https://doi.org/10.3390/s21062140>

[49] Jin Hyeok Yoo, Yecheol Kim, Jisong Kim, and Jun Won Choi. 2020. 3D-CVF: Generating Joint Camera and LiDAR Features Using Cross-view Spatial Feature Fusion for 3D Object Detection. In *Computer Vision – ECCV 2020*, Andrea Vedaldi, Horst Bischof, Thomas Brox, and Jan-Michael Frahm (Eds.). Springer International Publishing, Cham, 720–736.

[50] Ziyuan Zhong, Gail Kaiser, and Baishakhi Ray. 2021. Neural Network Guided Evolutionary Fuzzing for Finding Traffic Violations of Autonomous Vehicles. *arXiv preprint arXiv:2109.06126* (2021).

[51] Ziyuan Zhong, Yun Tang, Yuan Zhou, Vânia de Oliveira Neves, Yang Liu, and Baishakhi Ray. 2021. A Survey on Scenario-Based Testing for Automated Driving Systems in High-Fidelity Simulation. *CoRR* abs/2112.00964 (2021). arXiv:2112.00964 <https://arxiv.org/abs/2112.00964>

[52] Taohua Zhou, Mengmeng Yang, Kun Jiang, Henry Wong, and Dianne Yang. 2020. MMW Radar-Based Technologies in Autonomous Driving: A Review. *Sensors* 20, 24 (2020). <https://doi.org/10.3390/s20247283>

A BACKGROUND: CAUSALITY ANALYSIS

Over the recent years, causality analysis has gained popularity on interpreting machine learning models[13, 22]. Compared with traditional methods, causal approaches identify causes and effects of a model’s components and thus facilitates reasoning over its decisions. In the current work, we apply causality analysis to justify the defined fusion errors are indeed ADAS errors caused by the fusion method.

In causality analysis, the world is described by variables and their values. Some variables may have a causal influence on others. The influence is modeled by a set of *structural equations*. The variables are split into two sets: *the exogenous variables*, whose values are determined by factors outside the model, and *the endogenous variables*, whose values are ultimately determined by the exogenous variables. In our context, exogenous variables can be a user specified test design for an ADAS (e.g., testing the ADAS for a left turn at a signalized intersection scenario), the endogenous variables can consist of the configuration for the ADAS under test (e.g., the ego car’s target speed), the concrete scenario (e.g., the number and locations of the NPC vehicles), and the final test results (e.g., if a collision happen).

Formally, a causal model M is a pair (S, F) . S is called "signature" and is a triplet (U, V, R) . Among them, U is a set of exogenous variables, V is a set of endogenous variables, and R associates with every variable $Y \in U \cup V$ a nonempty set $R(Y)$ of possible values for Y . F defines a set of modifiable structural equations relating the values of the variables.

Given a signature $S = (U, V, R)$, a primitive event is a formula of the form $X = x$, for $X \in V$ and $x \in R(X)$. A causal formula (over S) is one of the form $[\vec{Y} \leftarrow \vec{y}] \phi$, where \vec{Y} is a subset of variables in V and ϕ is a boolean combination of primitive events. This says ϕ holds if \vec{Y} were set to \vec{y} . We further denote $(M, \vec{u}) \models \phi$ if the causal formula ϕ is true in causal model M given context $U = \vec{u}$. $(M, \vec{u}) \models (X = x)$ if the variable X has value x in the unique solution to the equations in M given context \vec{u} .

We next provide the definition of causality.

Definition 2. $\vec{X} = \vec{x}$ is an actual cause of ϕ in (M, \vec{u}) if the following three conditions hold:

AC1. $(M, \vec{u}) \models (\vec{X} = \vec{x})$ and $(M, \vec{u}) \models \phi$

AC2. There is a partition of V into two disjoint subsets \vec{Z} and \vec{W} (so that $\vec{Z} \cap \vec{W} = \emptyset$) with $\vec{X} \subseteq \vec{Z}$ and a setting \vec{x}' of the variables in \vec{X} such that if $(M, \vec{u}) \models (\vec{W} = \vec{w})$ then

$$(M, \vec{u}) \models [\vec{X} \leftarrow \vec{x}, \vec{W} \leftarrow \vec{w}] \neg \phi$$

AC3. \vec{X} is minimal; no subset of \vec{X} satisfies AC1 and AC2.

AC1 means both $\vec{X} = \vec{x}$ and ϕ happen. AC3 is a minimality condition. It makes sure only elements within \vec{X} that are essential are considered as part of a cause. Without AC3, if studying hard causes good grade then so is studying hard and being tall. AC2 essentially says when keeping everything else (except \vec{X} and those influenced by it) exactly the same, there is a \vec{x}' such that it can make ϕ does not hold.

In the current work, given an error happens (i.e., ϕ holds), we want to determine if the fusion method $(\vec{X} = \vec{x})$ is the actual cause. To achieve this, we want to identify scenarios such that AC1-AC3 are all satisfied. In fact, our defined fusion errors satisfy them.

Since \vec{X} only consists of one variable, the minimality condition AC3 is satisfied automatically. Given a collision scenario (i.e., ϕ is true), AC1 is also trivially satisfied with the fusion method \vec{x} used during the collision. The issue remains on how to achieve AC2, which is the main condition we analyze in Section 4.2.

B OTHER DETAILS OF FUSED

B.1 The objective for promoting fusion errors

F_{fusion} is formally defined as the percentage of the number of frames in which the fusion predicted lead having large deviation from the ground-truth lead, while at least one predicted lead from upstream sensor processing modules is close to the ground-truth lead:

$$F_{\text{fusion}}(x) = \frac{1}{|\mathbf{P}|} \times |\{i \mid \exists k \in \mathbf{K} \text{ s.t. } \|\hat{s}_{ik} - y_i\|_1 < th \text{ and } \|\hat{y}_i - y_i\|_1 > th \text{ and } i \in \mathbf{P}\}| \quad (2)$$

where \mathbf{P} is a set of indices of the frames during the pre-crash period, \mathbf{K} is a set of indices of the sensors, \hat{s}_{ik} is a predicted lead by sensor k at time frame i , \hat{y}_i is the predicted lead by the fusion component, y_i is the ground-truth lead and th is an error threshold. Note each lead variable here is three-dimensional (i.e. relative longitudinal distance, relative latitudinal distance, and relative speed) and each of them is scaled down (by 4m, 1m, and 2.5m/s, respectively, which are chosen based on domain knowledge as well as the empirical observations). th is set to 3 by default meaning the prediction at a frame is considered accurate only when none of the three predictions has large deviations from the ground-truth.

B.2 Selection.

We use binary tournament selection, as in previous work on testing ADAS [2]. For each parent candidate seed, the method creates two duplicates and randomly pairs up all the parent candidate seed duplicates. Each pair’s winner is chosen based on their fitness function values. The winners are then randomly paired up to serve as the selected parents for crossover.

B.3 Crossover & Mutation.

We use simulated binary crossover [7] as in [2]. We set the distribution index $\eta = 5$ and probability=0.8 to promote diversity of the offspring. We further apply polynomial mutation to each discrete and continuous variable with mutation rate set to $\frac{5}{k}$, where k is the number of variables per instance, and the mutation magnitude $\eta_m = 5$ to promote larger mutations.

C RADAR IMPLEMENTATION FOR OPENPILOT IN CARLA

The official OPENPILOT bridge implementation does not implement radar in the simulation environment. To evaluate the fusion component of OPENPILOT, we create a radar sensor in CARLA following Delphi Electronically Scanning RADAR [40] (174m range and 30 horizontal degrees) and send processed radar data at 20Hz. Since

the radar interface in CAN of OPENPILOT takes in pre-processed 16 tracks including relative x, relative y, and relative speed, the raw radar information in CARLA is pre-processed using DBSCAN [18] (with $\text{eps} = 0.5$ and $\text{min samples} = 5$), a widely used for raw radar data pre-processing [52].

D SETTINGS FOR CARLA AND CHANGES MADE ON OPENPILOT FOR IMPROVED SIMULATION DETERMINISM AND REPRODUCIBILITY

By default, the communications among CARLA client (OPENPILOT in our case), traffic manager (controlling NPC vehicles), and CARLA server (controlling the world environment) use asynchronous communication. The CARLA world also has a non-stationary "time step" between every two updates. In particular, the virtual time between two updates of the world is set to be equal to the real-world computing time. Besides, OPENPILOT is a real-time system and its internal communications among its modules are asynchronous. These default designs introduce non-determinism to a simulation's result which becomes dependent on the underlying system's state. This also makes reproducing an accident of OPENPILOT in CARLA very difficult.

To conquer these difficulties, we apply the following configuration settings and changes. Note that for simplicity, in the current work, we collectively call the changes we have made as setting the CARLA communication configurations and the OPENPILOT communication configurations to be deterministic and synchronous.

First, we adopt synchronous mode for CARLA and CARLA TRAFFIC MANAGER, set a random seed to 0 for CARLA TRAFFIC MANAGER, and use a fixed virtual time step of 0.01 seconds. These allow the scenarios created to be deterministic. Second, we adopt some design choices of Testpilot[37] which was developed based on OPENPILOT 0.5 (a very early version) and achieved complete synchronization between CARLA and OPENPILOT. In particular, we modify OPENPILOT to use the simulator's virtual time passed from the bridge between the simulator and the controller rather than using the real world time. Besides, we modify the communication among the modules inside OPENPILOT to be synchronous. Note that if OPENPILOT uses real time, CARLA will be not able to catch up with the speed of OPENPILOT and thus lead to significant communication delay. What's more, before each scenario starts, we allow OPENPILOT to take in sensor input from CARLA for 4 virtual seconds to allow all of its modules up and running. This step is necessary since on different machines, it takes different virtual time for OPENPILOT to start all the modules. With these changes, the simulation is more deterministic, and fusion errors can be easily reproduced across runs and machines.

One caveat is that because of all these changes made, although we try the best to make reasonable changes, it is still possible that some of the crashes reported here may not happen on a specific vehicle controlled by OPENPILOT (which uses asynchronous communication) in the real world.

E ADAPTION OF MATHWORK RADAR-CAMERA FUSION

The original Mathwork implementation is in Matlab, we reimplement it in Python. Besides, the Mathwork implementation uses an Extended Kalman Filter since the radar measurements are non-linear. Since OPENPILOT takes a transformed linear radar measurements (i.e. the relative position is in the Cartesion coordinate rather than angular coordinate), we use a Linear Kalman Filter instead. Besides, the speed of y axis (in terms of the ego car's coordinate) is not supported by the OPENPILOT interface so we leave this field as a constant in the Kalman Filter modeling. These changes can potentially introduce fusion errors that may not appear in the original implementation.

F SEARCH SPACE DETAILS

Lighting condition is controlled by sun azimuth angle and sun altitude angle. Weather consists of the following fields: cloudiness, precipitation, precipitation deposits, wind intensity, fog density, fog distance, wetness, and fog falloff, the detailed explanation of each field can be found on CARLA Python API [17].

Each NPC vehicle has a model type field and five waypoints, each of which consists of two fields (speed and changing lane). Thus each NPC vehicle has 11 ($= 1 + 5 * 2$) dimensions to search for. In each scenario, the search space has 76 dimensions since it has six NPC vehicles ($6 * 11 = 66$ searchable fields), two searchable lighting fields, and eight searchable weather fields.